Electronic Supplementary Information (ESI†)

Mechanochemical ZIF-9 Formation: In Situ Analysis and Photocatalytic Enhancement Evaluation

Noelia Rodríguez-Sánchez[1,2], Carsten Prinz[1], Ralf Bienert[1], Menta Ballesteros[2,3], A. Rabdel Ruiz Salvador[2,4], Biswajit Bhattacharya[1]*, Franziska Emmerling[1,5]*

*Corresponding authors: BB biswajit.bhattacharya@bam.de and FE franziska.emmerling@bam.de

[1]BAM Federal Institute for Materials Research and Testing, Richard-Willstätter-Straße 11, 12489, Berlin, Gemany.

[2]Center for Nanoscience and Sustainable Technologies (CNATS), Universidad Pablo de Olavide, Ctra. Utrera km. 1, 41013, Seville, Spain.

[3]Department of Molecular Biology and Biochemistry Engineering, Universidad Pablo de Olavide, Ctra. Utrera km. 1, 41013, Seville, Spain.

[4] Department of Physical, Chemical and Natural Systems, Universidad Pablo de Olavide, Ctra. Utrera km. 1, 41013, Seville, Spain.

[5]Department of Chemistry, Humboldt-Universität of Berlin, Brook-Taylor-Strasse 2, 12489 Berlin, Germany.

Content

Study of adsorption kinetics models……..3

Figure S.1 X-Ray Diffraction data for mechanochemical and solvothermal ZIF-9……...…3

Figure S.2. X-Ray Diffraction data of NH_4Cl concentration evaluation in mechanochemical ZIF-9……4

Figure S.3. X-Ray diffraction data for solvent evaluation in mechanochemical ZIF-9…….....…4

Figure S.4. X-Ray diffraction data for different shaker milling instruments……..5

Figure S.5. X-Ray diffraction data in large scale of mechanochemical ZIF-9…….….5

Figure S.6. Adsorption isotherms for solvothermal synthetized and mechanochemical ZIF-9…….6

Table S.1. BET data of solvothermal and mechanochemical ZIF-9…….……..6

Figure S.7. EDS data for solvothermal and mechanochemical synthetized ZIF-9…….……..7

Figure S.8. MB degradation by photolysis and combined action of light and H_2O_2.……8

Figure S.9. MB adsorption models for mechanochemical ZIF-9.....9
Table S.2. Langmuir, Freundlich and Tempkin adsorption model parameters……...10
Figure S.10. Zero-order and pseudo-second order kinetics models for ZIF-9……..…….10
Figure S.11. Recyclability and first- order kinetic of mechanochemical synthesized ZIF-9…….11

Study of adsorption kinetics models

Langmuir, Freundlich, and Temkin adsorption models were analyzed for mechanochemical ZIF-9 based on the dark period during photo-Fenton test. The calculations of these analyses were based on the equations [1-3] corresponding to Langmuir, Freundlich and Tempkin isotherms respectively:

$$\frac{C_e}{q_e} = \frac{1}{q_{max}K_L} + \frac{C_e}{q_{max}} \quad \text{Eq.1}$$

$$\ln q_e = \frac{1}{n}\ln C_e + \ln K_F \quad \text{Eq.2}$$

$$q_e = K_T \ln f + K_T \ln C_e \quad \text{Eq.3}$$

Where q_e is the equilibrium adsorption capacity (mg g^{-1}), q_{max} is the maximum adsorption capacity (mg g^{-1}), and K_L and K_F are the Lagmuir and Freundlich constants, respectively. K_T and f (mg L^{-1}) are the Tempkin and binding constants, respectively.

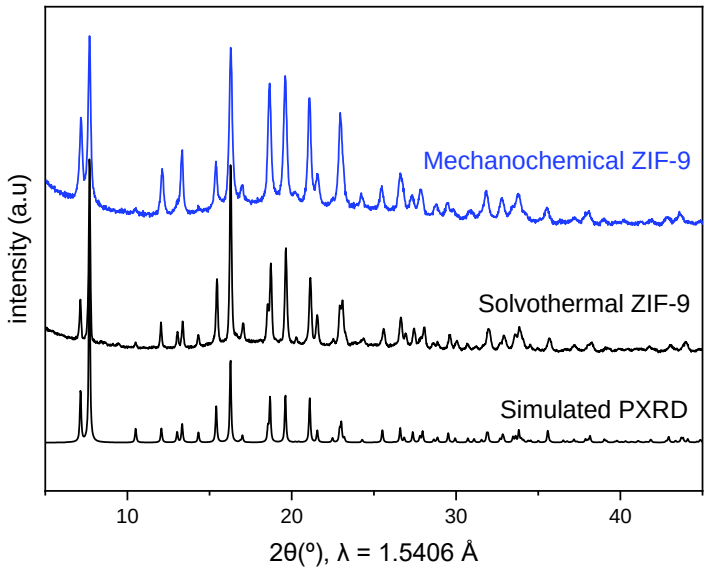

Fig. S.1. X-Ray Diffraction Patterns for solvothermal synthetized ZIF-9 (black) and mechanochemical synthetized ZIF-9 (blue).

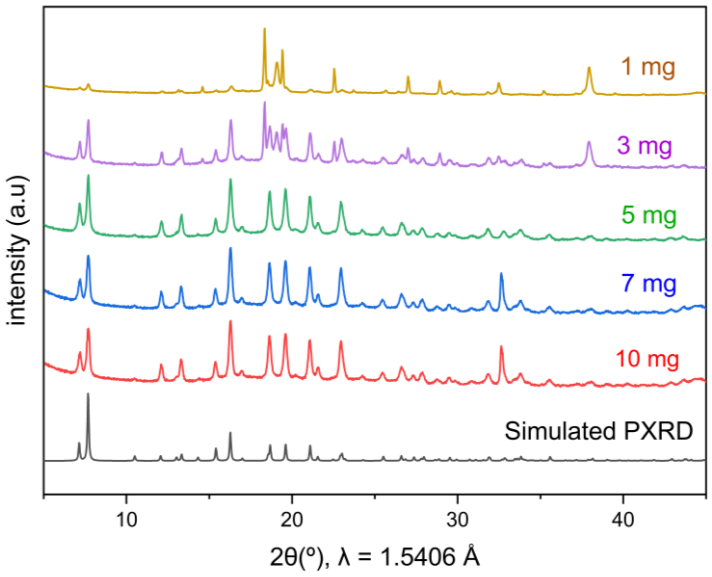

Fig.S.2. Evaluation of the concentration of NH_4Cl in the synthesis of mechanochemical ZIF-9.

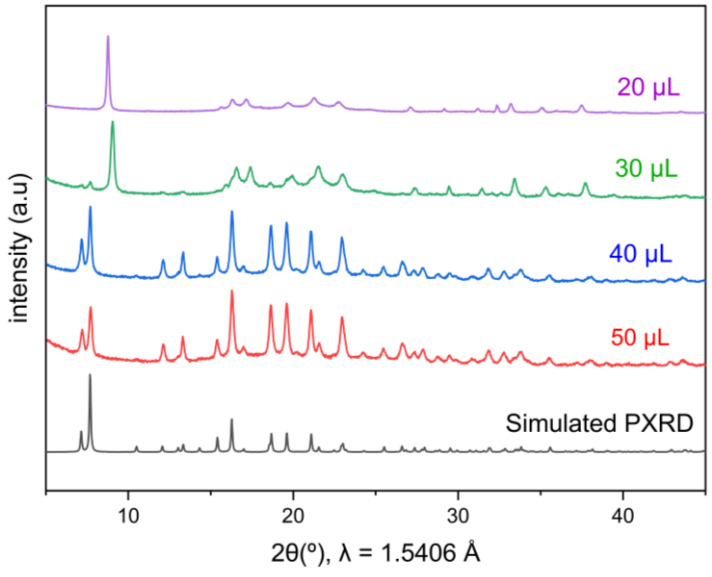

Fig. S.3. Evaluation of the concentration of DMF in the synthesis of mechanochemical ZIF-9.

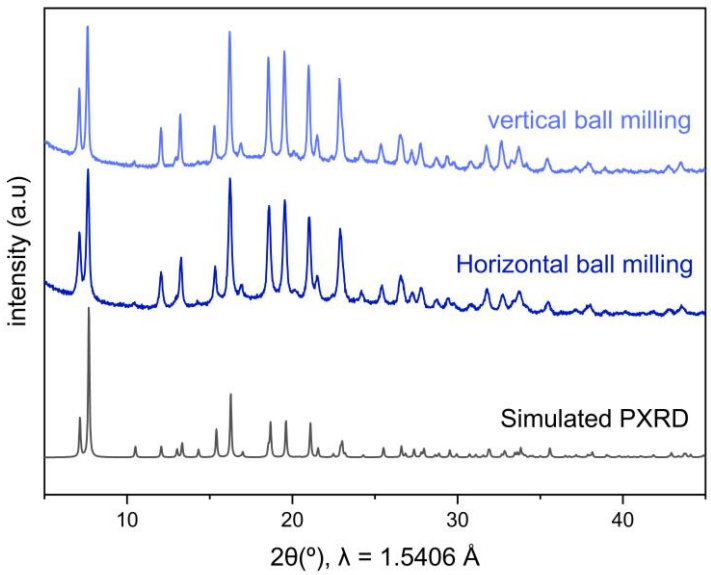

Fig. S.4. X-Ray diffraction patterns for mechanochemical ZIF-9 using a shaker mill with a vertical movement (light blue) and with horizontal movement (dark blue).

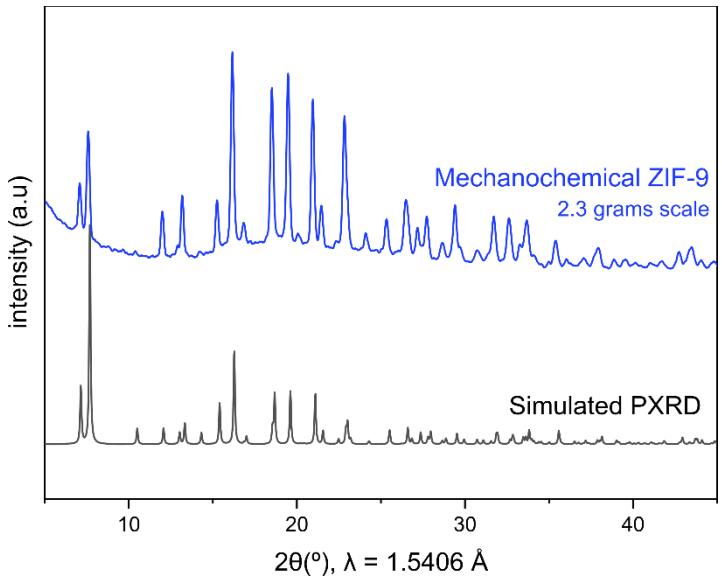

Fig. S.5. X-Ray diffraction patterns for 2.3 grams scale of mechanochemical ZIF-9.

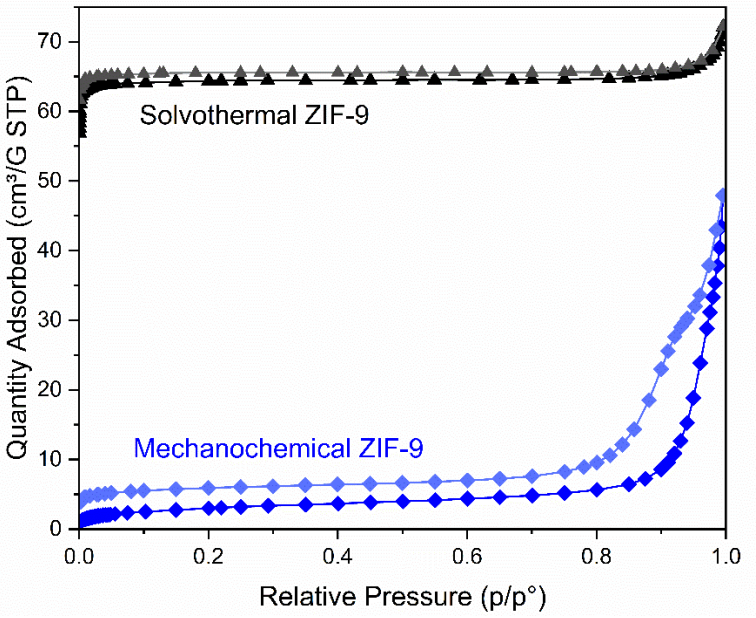

Fig.S.6. Adsorption isotherms for solvothermal synthetized ZIF-9 (black) and mechanochemical synthetized ZIF-9 (blue).

Table S.1. Specific surface area (BET) analysis of solvothermal and mechanochemical ZIF-9.

Material	Specific surface area (BET) [m²/g]	Uncertainty (BET) [m²/g]	C	Cor. Coeff.	Measuring [p/p$_0$]
Solvothermal ZIF-9	274.06	± 0.0652	18839	0.9999	0.00108 - 0.00478
Mechanochemical ZIF-9	10.93	±0.0298	76.079	0.9999	0.05554 – 0.21977

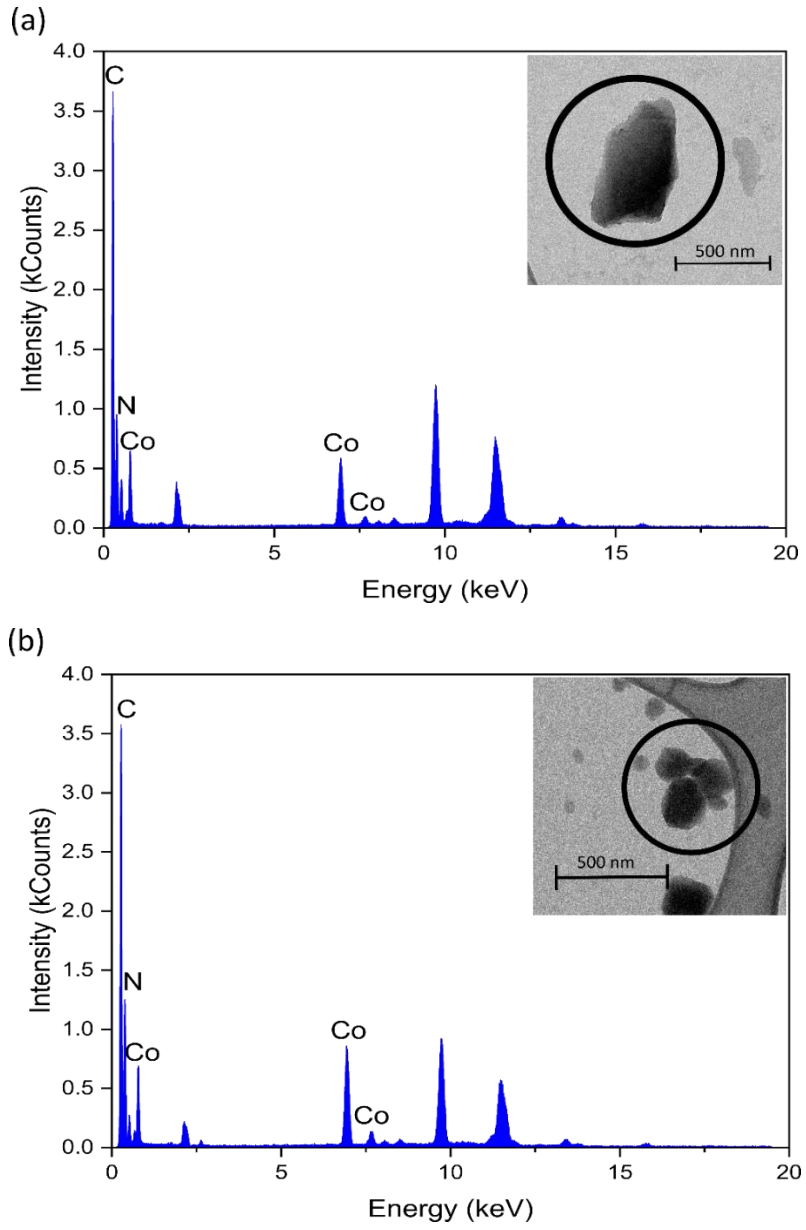

Fig.S.7. EDS spectra for solvothermal synthetized ZIF-9 (a) and mechanochemical synthetized ZIF-9 (b).

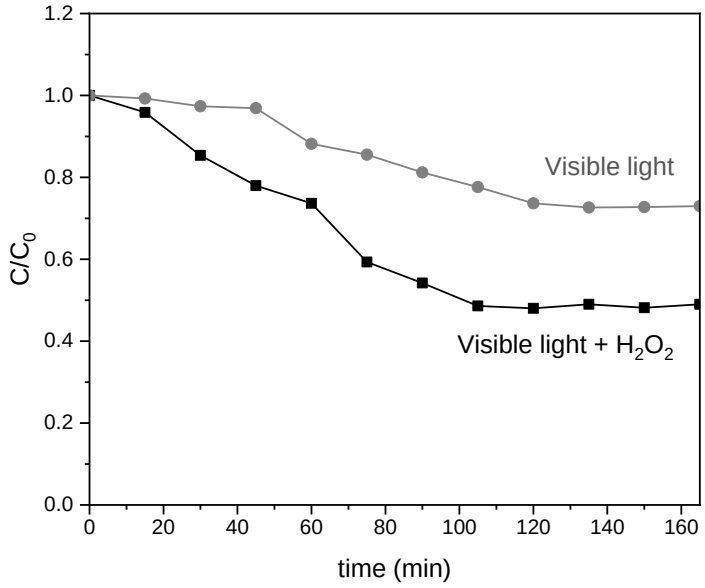

Fig.S.8. Methylene blue degradation by influence of visible light (grey) and the combined action of visible light and H_2O_2 (black).

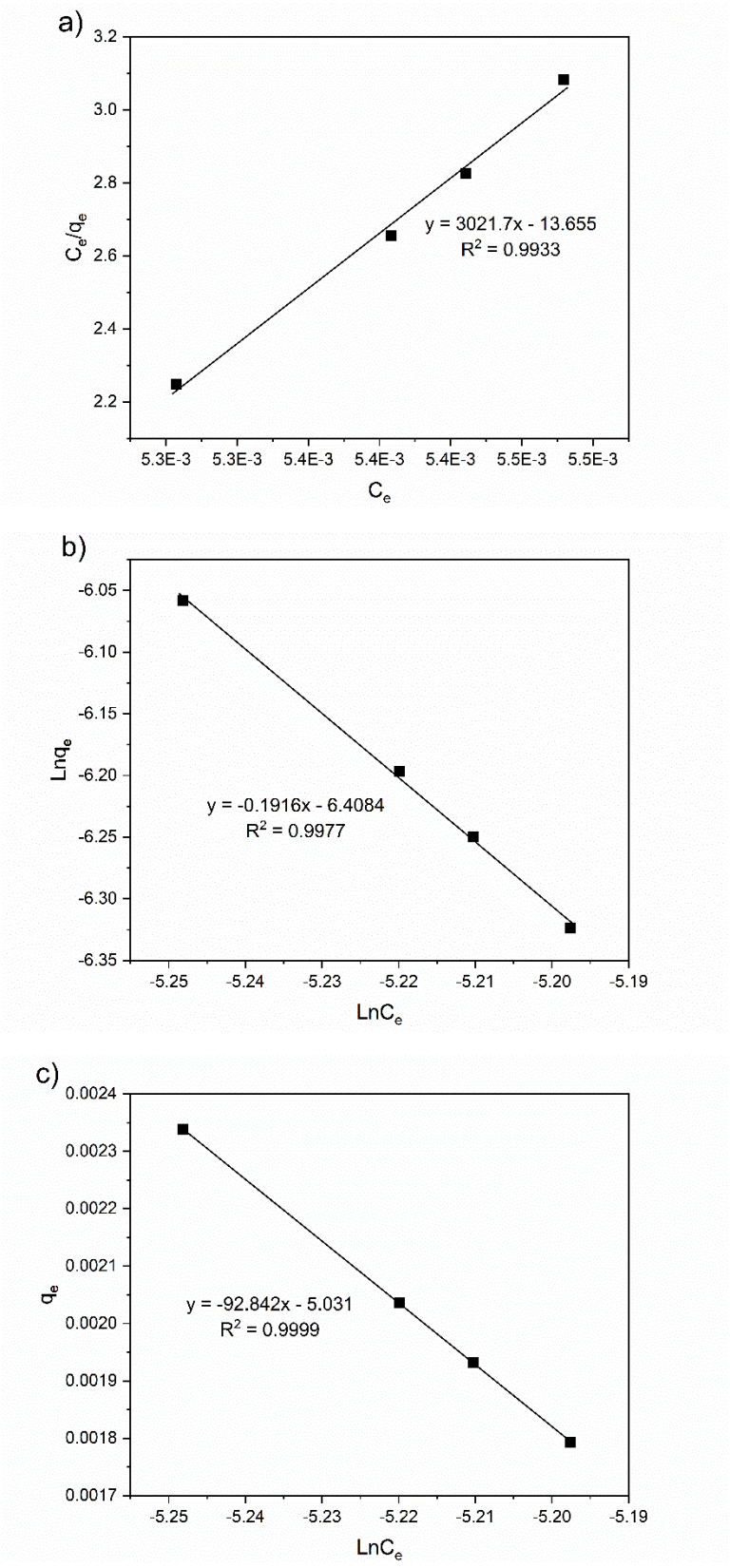

Fig. S.9. MB adsorption on mechanochemical synthesized ZIF-9 based on a) Langmuir, b) Freundlich and c) Tempkin isotherms.

Table S.2. Langmuir, Freundlich and Tempkin model parameters for mechanochemical synthetized ZIF-9.

Langmuir K_L (L mg^{-1})	q_e (mg g^{-1})	R^2	Freundlich K_F [(mg g^{-1}). (L mg^{-1}) $^{1/n}$]	n	R^2	Tempkin K_T (L mg^{-1})	f	R^2
-2.213E+02	3.309E-04	0.9933	0.001648	-5.21921	0.9977	-92.842	1.05568	0.9999

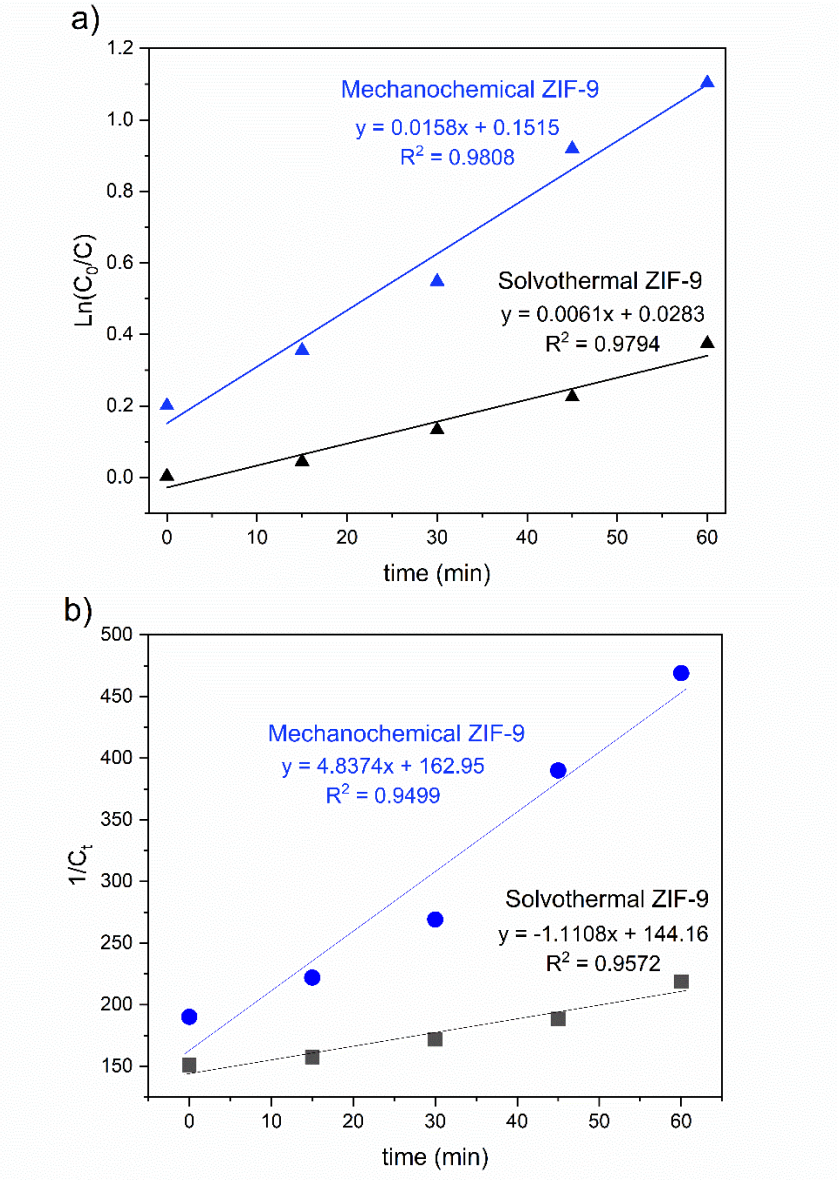

Fig.S.10. Zero-order (a) and pseudo-second order (b) kinetics for solvothermal synthetized ZIF-9 (black) and mechanochemical synthetized ZIF-9 (blue)

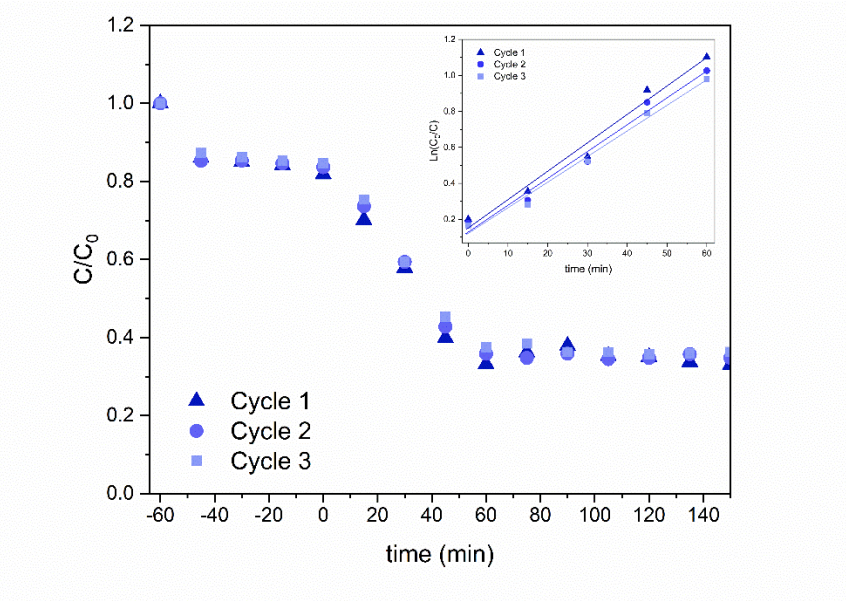

Fig. S.11. Recyclability and first- order kinetic of mechanochemical synthesized ZIF-9 over three cycles.